Spatial size of waves

Podgórski, Krzysztof; Rychlik, Igor

2016

Working Papers in Statistics
No 2016:3

Department of Statistics
School of Economics and Management
Lund University

Spatial size of waves

KRZYSZTOF PODGÓRSKI, LUND UNIVERSITY

IGOR RYCHLIK, CHALMERS UNIVERSITY OF TECHNOLOGY

Spatial size of waves

KRZYSZTOF PODGÓRSKI* AND IGOR RYCHLIK**
Addresses:
* Department of Statistics, Lund University, SE-220 07 Lund, Sweden
podgorski@lu.se
** Mathematical Sciences, Chalmers University of Technology, SE-412 96 Göteborg, Sweden
rychlik@chalmers.se

Abstract: A method of measuring three-dimensional spatial wave size is proposed and statistical distributions of the size characteristics are derived in explicit integral forms for Gaussian sea surfaces. New definitions of wave characteristics such as the crest-height, the length, the size and the wave front location are provided in fully dimensional context. The joint statistical distributions of these wave characteristics are expressed in the terms of a directional power spectrum. The proposed approach allows for investigation of the influence of spectral shape and directionality on the joint distributions of the size characteristics. The method is validated by comparing numerical evaluations of the distributions with the observed frequencies extracted from simulations of sea surface. The comparisons demonstrate high accuracy of the obtained distributions.

Keywords: Gaussian fields, Rice formula, sea surface, directional spectra, wave statistics, wave crest, wave crest length, wave size.

1 Introduction

In oceanography and marine technology the sea elevation seen as a three dimensional moving surface is perceived as propagating trains of apparent waves. Determination of statistical properties of three dimensional wave sizes is of great importance in ocean-engineering applications such as a design of mechanical structures that have dimensions of the same order of magnitude as the wave, e.g., oil platforms, wave energy harvesters, or even floating airports, bridges, large ships and piers. However, while for waves measured along univariate directions the methodology is well-developed, see for example [22], [18], among many others, the fully three dimensional approach is rarely tackled. The lack of proper and operational definitions of three dimensional apparent waves and their dimensional characteristics should be mostly blamed for this state of affairs. The importance of developing methodology to address this problem lies in the fact that the impact of a wave on a structure depends on the wave shape in space. Currently, this shape is often characterized by the wave-length and the crest height (or amplitude) and the wave-length distribution became important information for the design of structures. The problem with this approach is in its restriction to the sea surface observed along a line. Hence it does not fully describe the size of a wave in space except for a long-crested sea. In this paper we introduce an extended approach that captures better three-dimensional spatial waves. This approach is based on new definitions of wave sizes and on the Rice's formula that facilitates derivation of their statistical distributions.

Through deriving the statistical distribution of large spatial waves one can help determine their damaging long-term effect on a structure. However truly large wave are rare and hence special care have to be taken to obtain frequencies of their appearances. Typically, the so called long-term (most often yearly) distribution of wave characteristics describing wave variability during decades is of the main interest. The wave climate in the region can be used to deduce the long-term distribution at a given location of interest. Unfortunately, only temporal measurements at a location are most often available which requires transforming temporal wave characteristics, e.g. crest height and period, into spatial ones may lead to inadequate results, see [17]. This is due to the fact that from temporal records one can estimate the spectrum but not the directional spectrum which influences the distributions of spatial wave characteristics. This can be also seen in examples at the end of the paper. To improve accuracy one can use wave climate models and/or directional buoys measurements [4], that may provide with

spectral characterization of sea spatial conditions.

More specifically, for a fixed directional spectrum one could use Fourier transform and apply the dispersion relation on a per sine wave component basis, as shown in [21], to derive spatial (or spatio-temporal) sea elevation surfaces $W(x, y, t)$ and then estimate the distribution of wave characteristics of interest associated with the particular spectrum, see [10] for introduction the probabilistic sea state modeling. This spectrum however is changing over longer periods although at a much slower rate than the variability of waves. To account for such a slow long term variability of spectra, one can introduce varying parameters in the spectra. Eventually the long-term distribution is obtained in two steps. First deriving the distributions for a stationary sea state corresponding to a short-term wave climate condition. Then averaging these distributions over the climate, i.e. over the long-term distribution of the spectra parameters.

This estimation of the stationary state distribution can be based on simulations of large number of fields, using a directional spectrum associate with the instantaneous (short term) wave climate at the location. Then the long-term distributions of some wave characteristics from those simulations are obtained by averaging simulation for various spectra related to the wave climate variability. However the computation cost of such a procedure would be prohibitive, especially if one wants good accuracy for high - and thus rare - crests. In this paper we demonstrate a method of direct estimation of the short-term distributions using the probabilistic model of W for a given directional spectrum. Through this we avoid simulations of large fields that are required to statistically capture rare extreme events.

The paper is organized as follows. Section 2 contains introductory material: notation, definitions of wave characteristics in one dimensional records, and a short review of distributions of wave characteristics in Gaussian seas. The new findings, definitions of wave characteristics of waves in sea surface, are given in Section 3. This section concludes with Subsection 3.3, which contains a short discussion of methods that are used for evaluation of statistical distribution of the proposed waves characteristics. It serves as an introduction to the results given in Appendix II, where a number of mathematical formulas for wave characteristics distributions are given. Validation of the proposed methodology and some examples are presented in the two final sections: Section 4 is dealing with a spectrum corresponding to a long-crested sea and Section 5 where a spectrum typifying a confused (short-crested) sea is used. Conclusions and an extensive list of references follows. The two appendices that close the paper provide material that makes the presentation self-contained. In the first appendix the Gaussian sea is defined while the second one contains formulas for various wave characteristics distributions derived using Rice's formula for the intensity of marked zeros of random processes.

2 Distributions of waves characteristics along one dimension

Sea surface elevation is often measured at a fixed location and saved in the form of a time series. Here, we use time context although the measurements can be made linearly in the space as well in which the case some obvious modification of terminology is needed. The so called zero-crossing wave is used to define apparent waves. In this approach wave is a part of a record between two consecutive zero-upcrossings of the mean sea level. For simplicity it is assumed that the latter, also called the still water level, is set to zero. Important wave characteristics are crest height A^c and crest duration (half period of a wave) T^c, see Figure 1*(Left)*. The crest A^c of a wave is the maximum value between a zero-upcrossing and the following zero-downcrossing. Similarly, the crest duration T^c is the time distance between a zero-upcrossing and the following downcrossing.

Since spatial records are seldom available the spatial wave characteristics relays on mathematical modeling of sea surface dynamics. A simple model, that is used here, assumes that each sinus wave component travel independently at its own celerity. It can be shown that it results in a probabilistic assumption that states that $W(x, y, t)$ is a Gaussian field, see [10] for details. For a long-crested sea for which $W(x, y, t) \approx W(x, t)$ one often assumes that sinus waves travels with negative velocity and hence a zero upcrossings is chosen to mark the front of an apparent wave.

Space wave characteristics are defined in spatial signals $W(x) = W(x, 0, 0)$ and $W(y) = W(0, y, 0)$. In the signals, for example $W(x)$, one can identify the spatial apparent waves which are characterized by its crest A^c_x and crest length L^c_x which is the distance between upcrossing and the following down-

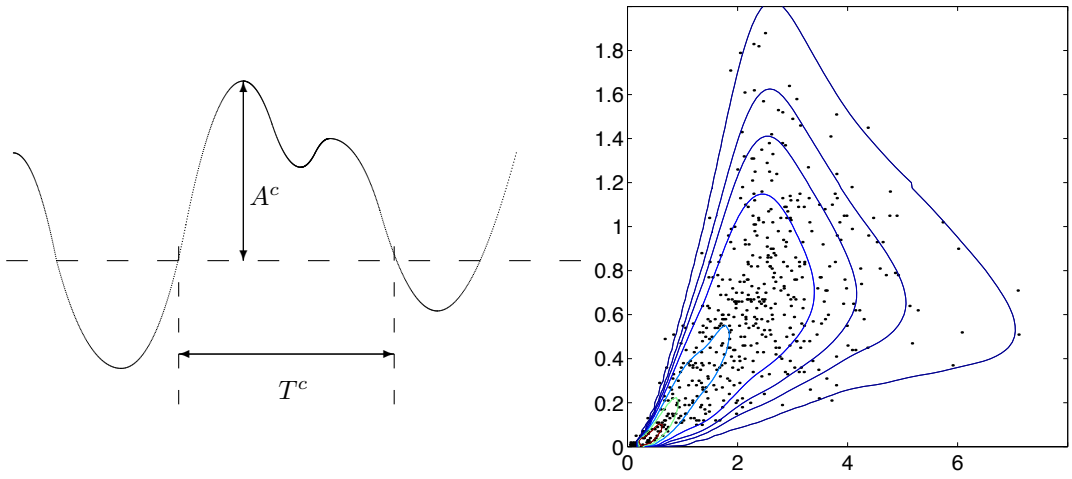

Figure 1: *Left:* The definition of wave wave crest A^c (crest amplitude) and half period (crest length) T^c. *Right:* The distribution of crest amplitude and length computed based on the Rice formula and the actual values observed in records of 534 temporal waves at shallow water of the coast of Africa.

crossings of the zero level. The characteristics A_y^c, L_y^c are defined in a similar way for waves in the spatial signal $W(y)$. In the following for simplicity of notation we will write A, L_x and L_y for crest height and crest lengths in x, y, directions, respectively.

Short term distributions describe variability of the observed waves during stationary sea conditions. These are understood as limits of histograms, empirical cumulative distributions etc of wave characteristics, as observation time/region grow without bounds. The limiting distributions can depend on the considered populations of waves, i.e. the way waves are collected (counted) and on particular definition of an apparent wave characteristics. Consequently, when presenting a distribution of, for example, wave crest A, it is important to clearly specify how waves are counted and how the wave crest height is defined.

In some applications one may count waves in temporal records. However it is important to be aware that their characteristics are describing both time and spatial properties of a wave. Take, for an instance, a structure exposed to wave loads. Responses of the structure are related to the crests in the time history that pass by exactly at the structure position and spatial size of a wave. In such situation one is counting waves in time while L is the most important wave characteristics, see [27]. Another examples of studies of some space-time aspects of apparent waves can be found in [28], where joint distribution of T^c, L_x has been studied, and in [1], [2] where distributions for encountered waves overtaking a vessel were discussed. (The distributions were used in evaluations of risks for capsizing due to broaching in [14].) However those wave characteristics were treated in the one dimensional manner, i.e. spatial-temporal distributions discussed above were derived using univariate random processes – no random fields were directly needed. Our approach differs in this important aspect as it truly involves the field $W(x, y)$ already at the characteristic definition level. In Section 3 two methods of counting waves in $W(x, y)$ and defining their characteristics will be discussed.

Finding simultaneous distribution of A, T^c, L_x, L_y for a Gaussian sea is a challenging problem. Means to evaluate two-dimensional pdf of A, T^c and A, L_x for Gaussian wave models were extensively studied in literature. Here we mention only two works [15], [22] were different approaches were compared. MATLAB toolbox WAFO [9] makes the methods practically available. These three articles contain a more complete list of work in the area. Despite the diversity of definitions of the wave populations and, consequently, of their wave characteristics, the generalized Rice's formula [23], [24], [29] can be used to evaluate the probability density functions (pdf) of the latter. In Figure 1*(Right)*, we have illustrated the approach by showing the isolines of the distribution for the crest amplitude and length computed used the JONSWAP spectrum (a popular class of spectra in ocean engineering) with the parameters fit to the empirical records. This distribution is compared with empirical distribution of

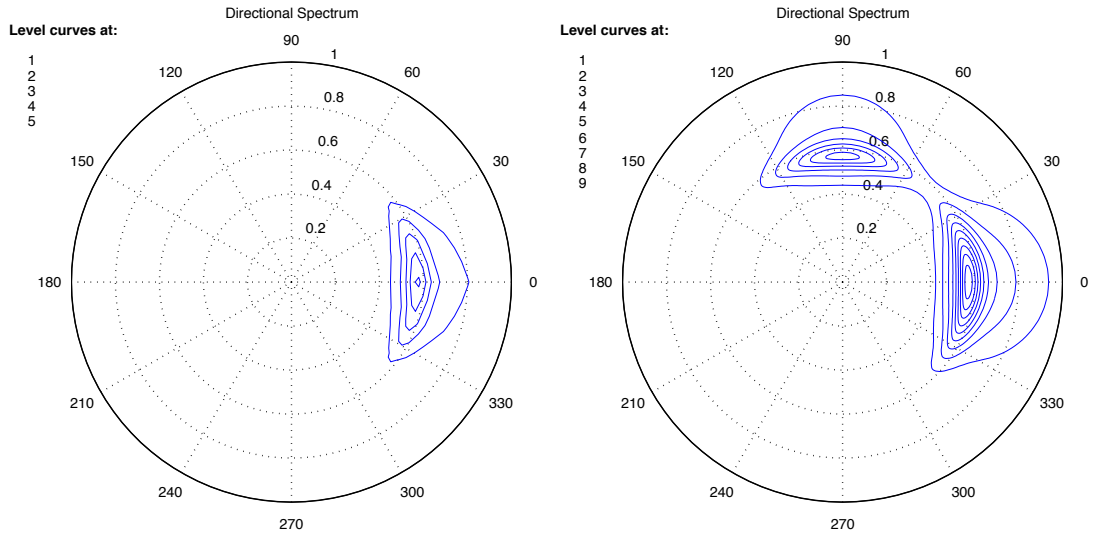

Figure 2: The directional spectra used in the examples. *Left:* Symmetric spectrum. *Right:* Asymmetric spectrum made of two wave systems propagating in different dirrections.

the amplitudes and lengths observed in the data (dots). One can notice that among 534 waves used in this example only very few are observed in the area of the extreme crest amplitudes and lengths. In contrast, the distribution based on Rice formula provides quite accurate density of the distribution also in regions with very few observations. This data set and the numerical routines for obtaining the figure can be found conveniently in the WAFO toolbox, [9]. See Appendix II for more examples.

3 Geometry of waves in space

In this section, two methods of counting waves are introduced and then used to define waves characteristics for the sea surface $W(x, y)$ that is located in three dimensions. The first one is a generalization of the zero-crossing waves, shown in Figure 1*(Left)*, while the second is inspired by approach presented in [27] where a concept of "acting wave crest" was introduced. The approaches coincide with one dimensional counterparts for long-crested sea, e.g. when all cosine waves are traveling mostly along the x axis. We remark here that the approach extends also to one more dimension – time. However, this important extension is not investigated in the presented work and is left for future studies.

A stationary Gaussian sea is fully characterized by a directional spectrum $S(\omega, \alpha)$ which describe energy of waves moving along a line having angle α with x axis. The frequency ω is observed in the time records and is carried out to the spatial records through the dispersion relation. In some maritime applications the direction α is essential for safety/risk evaluations. For example, for some structures rate of fatigue accumulation process depends on the angle α, see e.g. [11]. The methodology will by illustrated for waves defined in Gaussian sea $W(x, y)$ having directional power spectrum shown in Figure 2 *(Left)*. The spectrum has following parameters; significant wave height $h_s = 7$ [m], average crest length in x and y directions $E[L_x], E[L_y]$, defined in (3), equal to 21π [m] and 58π [m], respectively. In fact, the spectrum is a directional spread of a member from the JONSWAP parametric family of sea spectra with the half-time period equal to $E[T^c] = 4.7$[s].

3.1 Defining waves in space

We turn now to the first method of counting waves. Suppose one has chosen a fixed location, i.e. a position of a platform or a buoy. Let attach the coordinate system to the position. Consequently it can be of interest to study variability of apparent waves characteristics in space seen from this fixed position,

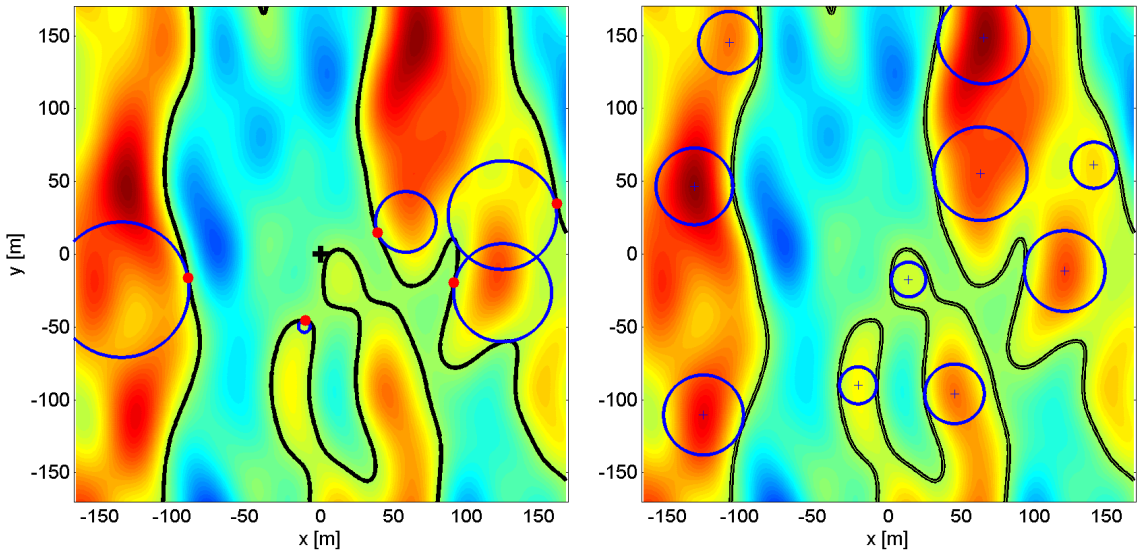

Figure 3: Illustrations of wave definitions given in Definition 1 (left plot) and in Definition 2 (right plot). The dark cross in the left hand side graph marks the origin while the crosses on the right sand one mark the local maxima.

i.e. from the orign. The following definition of a wave front (related to the the platform position), the crest height and length mathematically describes the wave for this reference point.

Definition 1. *A point* $\mathbf{q} = (x, y)$ *is a front of a wave if the sea is at the zero level at it and the direction to this point from the origin coincides with the direction of the gradient of* W *at* $\mathbf{q}$*. Formally,* $W(\mathbf{q}) = 0$ *and for a positive constant* λ

$$\mathbf{q} = -\lambda \left(W_x(\mathbf{q}), W_y(\mathbf{q})\right) \tag{1}$$

where $(W_x(\mathbf{q}), W_y(\mathbf{q}))$ *are the partial derivatives of* W *at* $\mathbf{q}$*, see Figure 3 (left plot) for an illustration.*

Let $\mathcal{D}$ *be the largest disk such that the front wave* $\mathbf{q}$ *is in* $\mathcal{D}$ *and that* W *is positive in the interior of the disk. The radius* R *of the disk defines the half length of waves crest while the height of the crest is defined as* $A = \max_{\mathbf{q}\in\mathcal{D}} W(\mathbf{q})$.

We turn now to the second, "global" and homogeneous method of counting waves, referred to in such a manner because our reference point is no longer associated with the origin but with any positive local maximum of sea surface wave.

Definition 2. *Point* $\mathbf{p}$ *is a center of a wave if* $W(\mathbf{p}) > 0$ *and* W *has local maximum at* $\mathbf{p}$*. The crest height of the wave is defined as* $A = W(\mathbf{p})$.

Let $\mathcal{D}$ *be the largest disk centered at* $\mathbf{p}$ *such that* $W(\mathbf{q}) > 0$ *for all* $\mathbf{q}$ *lying in the interior of the disk, see Figure 3 (right plot) for illustration. Then the radius* R *of* $\mathcal{D}$ *defines the half-length of the crest, while point* $\mathbf{q}$ *where the disk* $\mathcal{D}$ *is tangential to the zero level is a front of the wave. Further the angle* Θ *such that* $\mathbf{q} = \mathbf{p} + R(\cos\Theta, \sin\Theta)$ *will be called the direction of the front of the wave (with respect to the location of the crest).*

Important difference between the definitions is that the first one is local in the sense that one is selecting waves that could be relevant for an observer located on a platform. It seams that characteristics of the closest wave to the origin (observer) could be the most interesting one. Waves with fronts far away from an observer will change its shape (or even disappear) before reaching the observer. The distribution of the distance to the closest wave front will be considered in this paper. In contrast to the first definition, the second one, applied to a stationary sea, would locate waves homogeneously on

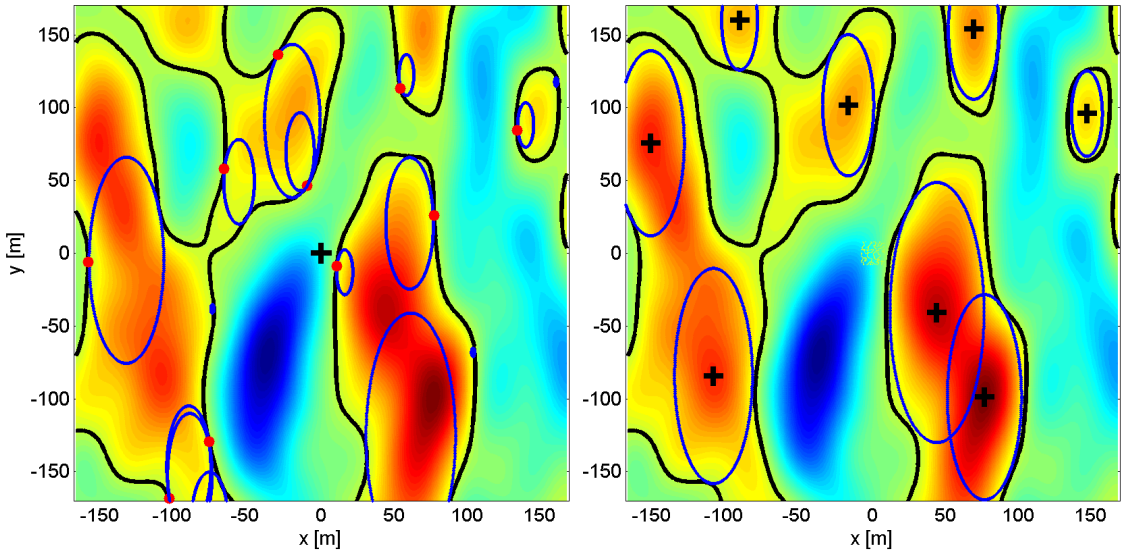

Figure 4: Size of waves in $W(x, y)$ by applying Definition 1 (left plot) and defined in Definition 2 (right plot) to the normalized field $\widetilde{W}(x, y)$.

(x, y)-plane. This is convenient when statistical properties of waves observed over a large area are of interest.

3.2 Size of a wave

The sizes of disks $\mathcal{D}$, given in Definitions 1 and 2, could serve as a proxy of the spacial spread of an apparent wave. However real waves are seldom isotropic, see Figure 3, and hence disk maybe inadequately describe the spread of a wave. Instead, we propose to use appropriate ellipses instead of circles and to introduce them we need to define the normalized sea surface.

3.2.1 The normalized sea surface

Consider a stationary sea with directional spectrum $S(\omega, \alpha)$, see Appendix I for details. The normalized sea surface $\widetilde{W}$ is obtained from W by scaling it in both arguments and in value so that $\widetilde{W}$ has variance and variances of its partial derivatives equal to one. This scaling has natural interpretation in terms of the normalized directional wave lengths as discussed next. It is defined using spectral moments λ_{ij} that are given by

$$\lambda_{ij} = \int_0^{2\pi} \int_0^{+\infty} S(\omega, \alpha) \left(\frac{\omega^2}{g}\right)^{i+j} (\cos\alpha)^i (\sin\alpha)^j \, d\omega \, d\alpha. \tag{2}$$

The significant wave height is then $h_s = 4\sqrt{\lambda_{00}}$ while

$$E[L_x] = \pi\sqrt{\lambda_{00}/\lambda_{20}} \qquad E[L_y] = \pi\sqrt{\lambda_{00}/\lambda_{02}} \tag{3}$$

are the average half wavelengths in x, y directions, respectively. With this notation and terminology the normalized field can be written explicitely

$$\widetilde{W}(x, y) = W\big(xE[L_x]/\pi, yE[L_y]/\pi\big)/\sqrt{\lambda_{00}}. \tag{4}$$

Thus the normalized sea has the half-lengths of the zero crossings waves both in the direction x and the direction y equal to π.

3.2.2 Size of a wave - area enclosed by an ellipse

Suppose that, for a sea state, the directional spectrum is known. In such a case for a given sea surface $W(x, y)$ one can rescale it to obtain the normalized field $\widetilde{W}(x, y)$, defined in (4). Now using Definitions 1 or 2 one can identify waves in $\widetilde{W}$. The crest position and half-length of the ith wave is denoted by $\widetilde{p}_i$, $\widetilde{R}_i$, respectively. The circles with centers at $\widetilde{p}_i$ and radius $\widetilde{R}_i$ become ellipses in the original (x, y) coordinates, see Figure 4 for illustration. The size of ith wave can be gauged by the area enclosed by the ith ellipse, viz.

$$S_i = \pi \, L_x \, L_y \widetilde{R}_i^{\,2}. \tag{5}$$

3.3 Intensity of waves

In evaluation of safety of maritime operation, "dangerous" (potentially harmful) events are often defined using wave characteristics, e.g crest height, period (length), wave steepness etc. Estimates of risks involves computations of frequency of the so identified "dangerous" waves. In what follows we define precisely what is meant by frequencies of the waves. We start with some necessary notation.

Let consider stationary (homogeneous) sea which will be observed in a region Λ, say. In the region one will count waves. Denote by N_Λ number of waves found in Λ and let the number of waves for which an event B happens be denoted by $N_\Lambda(B)$. Waves and "dangerous" waves (as described by an occurrence of B for such a wave) are most often spread homogeneously over the surface. Consequently there is a constant $\mu(B)$, called intensity, such that the expected number of "dangerous" waves in Λ is equal the intensity of waves times size of Λ, viz.

$$E[N_\Lambda(B)] = \mu(B) \cdot \|\Lambda\|,$$

where $\|\Lambda\|$ is the size of Λ (length, area, volume, etc.). Obviously the intensity of waves μ, say, is equal to $\mu(B)$ for an event B which is always true. Finally, the probability of B is defined by

$$P(B) = \mu(B)/\mu. \tag{6}$$

The probability can be formally interpreted, for the ergodic seas, as a limit of an empirical frequency $N_\Lambda(B)/N_\Lambda$ as the size $\|\Lambda\|$ increases without bound.

For a given sea state intensity of waves μ is easy to estimate and is often included as one of sea state parameters. Hence, by (6), quantities $\mu(B)$ and $P(B)$ could be equivalently used. However if estimates of μ and $P(B)$ are taken from different sources one has to be cautious that the same definitions of waves were used when estimating the parameters.

In many applications intensities $\mu(B)$ of interest are very small comparing to the duration of a sea state. Consequently the intensities have to be extrapolated from the available data. Statistics and probability theory are a natural frameworks for such extrapolations. Another approach is to assume a stochastic model for sea surface variability and then compute the intensities using suitable probabilistic tools. One is often using a Gaussian model for the sea, see Appendix I for definition. In such a case the power spectral density (psd) of a sea state defines the model and one can (at least in principle) evaluate distributions of various wave characteristics and use those to estimate $\mu(B)$. In particular Rice's formula [12], [23] and [24] and its generalizations, see e.g. in [29], [5] and references therein, are very useful tools to evaluate $\mu(B)$.

In Appendix II, an introduction to Rice's method to compute intensities of waves μ and $\mu(B)$ is given. Dynamics of waves will not be considered here and we refer to [18] and [6] where the dynamics of sea wave was statistically described, e.g. a probability distribution of velocities of wave crests in $W(x, y, t)$ were presented.

4 Wave sizes distributions for a long-crested spectrum

In this section we illustrate the proposed characteristics of waves in space by presenting the probability density functions (marginal and joint) for; crest height A, crest half-length R, direction of wave front

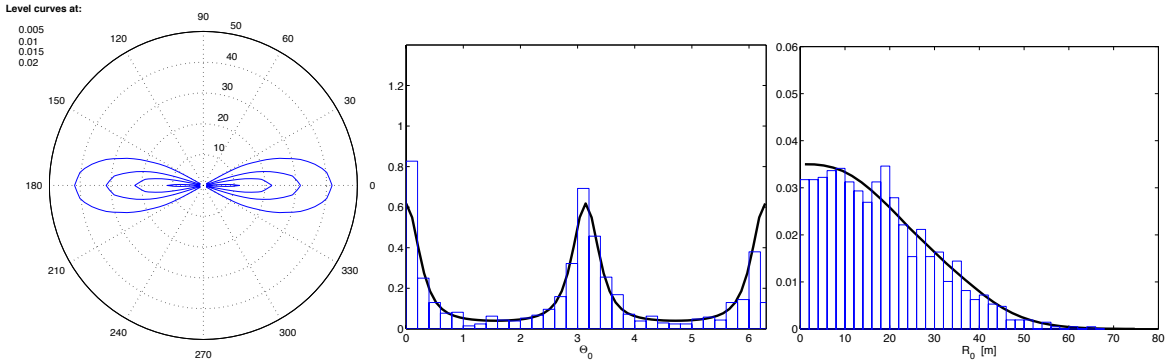

Figure 5: Distributions of size characteristics for waves that are closest to a fixed location (Definition 1) in the symmetric spectrum case presented in Figure 2 *(Left)*. *Left:* Joint probability density of R_0, Θ_0 plotted in the polar coordinates. The pdfs of Θ_0 *(Center)* and of R_0 *(Right)*, both obtained by integration from the joint pdf given in the left graph. They are compared with the histograms based on simulations.

Θ and the wave size S, for waves in a Gaussian sea having directional power spectrum shown in Figure 2 *(Left)*. The spectrum is defined by the following parameters; significant wave height $h_s = 7$ [m], average crest length in x and y directions $E[L_x], E[L_y]$, defined in (3), equal to 21π [m] and 58π [m], respectively. The formulas for wave intensities and probabilities or probability density functions (pdf) for various wave characteristics are given in Appendix II.

The presentation of the results is organized as follows. In the Section 4.1, the pdf for the location of the wave front, see Definition 1, that is closest to the observer, i.e. to the orign. The location is given in the polar coordinates (R_0, Θ_0), i.e. the wave front is located at $(R_0 \cos\Theta_0, R_0 \sin\Theta_0)$ in the Cartesian system. Next in Section 4.2, the pdf of (R, Θ), defined according to Definition 2, is computed. Note that the point $(R\cos\Theta, R\sin\Theta)$ is the location of a crest front when the orign of the coordinate system is placed at the location of a wave crest. In other words R is the distance to the closest wave front from a wave crest while R_0 was the distance to the closest wave front from a fixed point. Further in Section 4.3 computation of the probability that wave crest exceeds a fixed threshold is discussed. Then the joint pdf of (A, R, Θ), for waves defined in Definition 2, is presented in Section 4.4. Finally in Section 4.5 we show the pdf of size S of a wave.

4.1 Joint density of R_0, Θ_0.

Suppose that an observer is located at the origin, then a point $\mathbf{q} = R_0(\cos\Theta_0, \sin\Theta_0)$ is the position of the crest front closest to the observer. (Here wave front is defined according to Definition 1.) The formula (29) gives the pdf of R_0, Θ_0 in form of a high dimensional integral. Combining (29) and a suitable numerical integration algorithm allows for evaluation of the joint pdf of (R_0, Θ_0). For the directional spectrum, shown in the Figure 2 *(Left)*, the approximated density of R_0, Θ_0 has been derived and presented in Figure 5 *(Left)*. The polar coordinates have been used. The accuracy of the estimated is verified by using the marginal densities of R_0 and Θ_0, which are evaluated by means of a numerical integration of the joint density. The derived densities are shown in Figure 5 *(Center)* – R_0 and *(Right)* – Θ_0. The densities are compared with the normalized histograms of R_0 and Θ_0, respectively, found in simulated surfaces $W(x, y)$. One can see that histograms and pdfs $f_{R_0}(r)$, $f_{\Theta_0}(\theta)$ agrees very well. This illustrates the numerical accuracy of the WAFO software used to evaluate the pdf of R_0, Θ_0 given by (29).

4.2 Joint probability density of R, Θ

For comparison with the previous distribution we present the joint pdf of the (R, Θ) as described in Definition 2, i.e. when the reference point is located at the local maximum rather than at a fixed

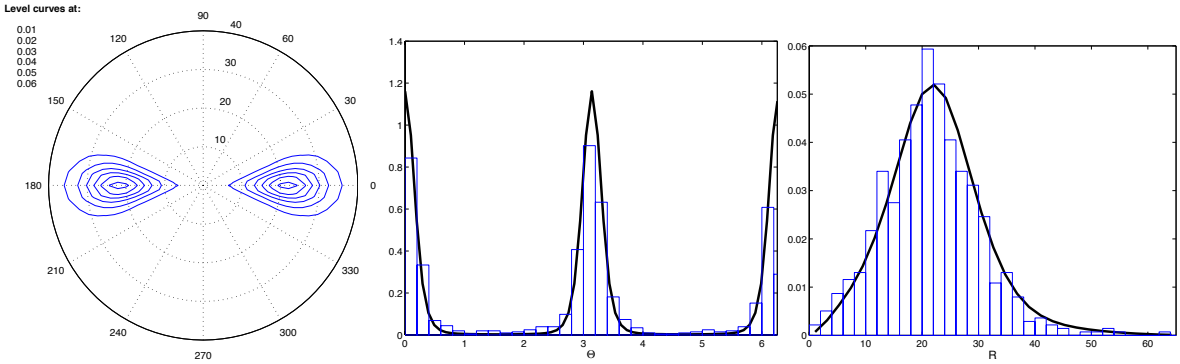

Figure 6: The analogous results to the ones presented in Figure 5 but for the case of wave size characteristics taken with the respect local maxima (Definition 2). *Left:* The joint pdf of R, Θ. *Center:* the pdf of Θ, compared with the normalized histogram. *Right:* the pdf of R. The marginal distribution are compared with the normalized histogram obtained from simulations.

location. The pdf is given by formula (28), which utilized the generalized Rice formula that takes into accounts the effect of randomly sampled local maxima. The wave characteristics (R, Θ) have been called the half-length of the crest and the direction of the wave front, respectively. The probability distribution of (R, Θ) has the following interpretation. Let place position of a randomly chosen wave crest at origin $(0, 0)$ and find the position $\mathbf{q}$ of the front of the wave. Then $\mathbf{q} = R(\cos\Theta, \sin\Theta)$.

The joint pdf of R, Θ is presented in Figure 6 *(Left)* in the polar coordinate system. The marginal pdfs of R, Θ are derived by means of numerical integration of the joint pdf and presented in Figure 6 *(Center)*– the azimuth Θ and in *(Right)* – the distance R. Both are compared for the accuracy check with the normalized histograms of R and Θ, respectively, found in simulated surfaces $W(x, y)$. One can see that histograms and pdfs $f_R(r)$, $f_\Theta(\theta)$ agree very well.

By examining Figure 5 and Figure 6, we may notice the main differences in the distributions of R_0, Θ_0 and R, Θ. Although both the wave characteristics describe distribution of the random location of the wave front: R_0 is the distance from an observer to the closest wave front while R is the distance from the crest of a wave to its wave front, we can see, as expected, that R_0 is more spread than R. This dependence is easily seen in the degenerated case when the sea surface consists of a single sine wave having wavelength L. In this case R_0 is uniformly distributed on $[-L/2, L/2]$ while R will be constant equal to $L/4$. This illustrates the intuitive fact that by locating the observation at a local maximum wave elevation is strongly correlated to maximum height. Moreover the angle Θ_0 varies much more than the angle Θ, while both have the mode at $0, \pi$ since the x axis is the main direction of wave propagation for the directional spectrum shown in Figure 2 *(Left)*. It shows that a level crossing contour at the front of a wave, when seen from the maximum is flatter in comparison with the one seen from the origin. It agrees with intuition in particularly for nearly long-crested seas.

4.3 Intensity of waves with crest exceeding a threshold

The intensity of waves in space can be measured in a variety of ways. One natural approach is through the intensity μ of the positive local maxima. The formula for this intensity is given in (23). For example, a Gaussian surface having spectrum given in Figure 2 *(Left)* has the (approximate) wave intensity $\mu = 0.85\,10^{-4}$ $[m^{-2}]$, ca. 1 [ha^{-1}], This approximation has been obtained by numerical evaluation of (23), while in see Figure 7 positive local maxima marked as white dots and their observed intensity per area unit represent empirical estimate of this intensity.

Often for practical reasons, the large crests are of principal interest and their intensity is represented by the intensity of crests exceeding h, $\mu(A > h)$, which is also given in (23). Estimates of $\mu(A > h)$ are often needed in evaluation of safety of maritime operations. There are possible some approaches

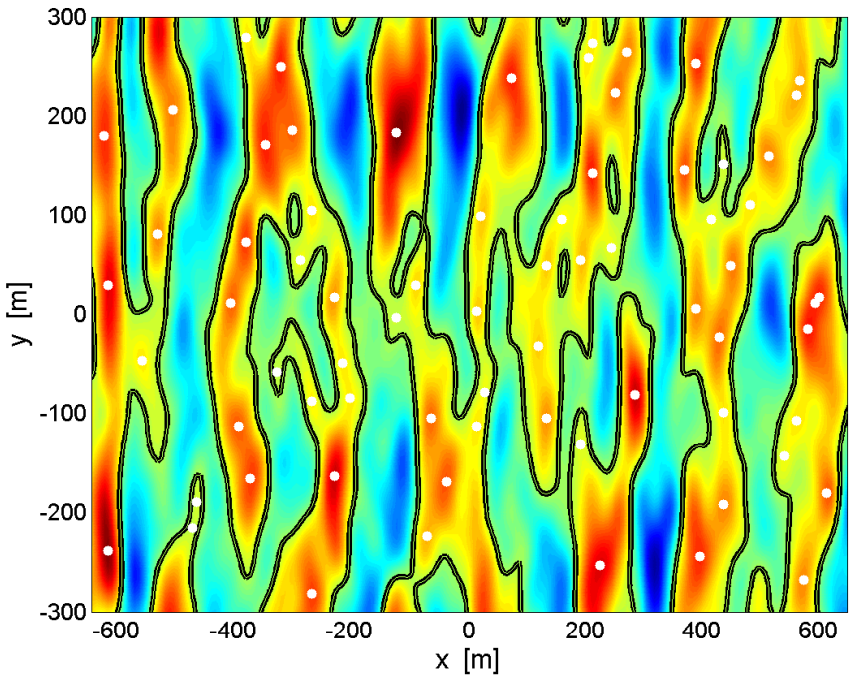

Figure 7: Simulation of a Gaussian sea having directional spectrum presented in Figure 2 *(Left)*. Intensity of waves tops is represented by positions of crests (positive local maximums) that are marked as white dots.

to get a more explicit although approximate form of the intensity. Here, we present an alternative approximation of the intensity employing (6), i.e. that $\mu(A > h) = \mu \cdot P(A > h)$. Since μ is already known, one needs only approximate $P(A > h)$. One can utilized for this purpose the distribution of A^c along linear record, defined in Figure 1 *(Left)*.

One could try to approximate the distribution of the crest height A^c, by means of the Rayleigh distribution that is applicable to the case when the sea is observed along the line. Then approximation states that $P(A^c > h) \approx \exp(-8\,(h/h_s)^2)$. Actually, for Gaussian sea $W(x)$ (or $W(t)$) the approximation is always conservative, see [26].

The logarithm of the intensity is shown in Figure 8 as solid lines. In this figure, the dashed lines are the approximation

$$\mu(A > h) \approx \mu \, \exp\left(-8\frac{h^2}{h_s^2}\right). \tag{7}$$

Although the Rayleigh bound was established for one dimensional record, it appears to work quite well even for the crest height distribution in $W(x, y)$ having the symmetric spectrum shown in Figure 2 *(Left)*. The error is less than 20 cm.

In [7] more detailed comparisons of extreme crest heights intensities for waves observed in time, space and in moving sea surfaces were presented, see also [5] and [19]. Among the results, a higher order approximation for the asymptotic distributions of the large wave heights in space has been presented that leads to the following approximation

$$\mu(A > h) \approx \mu \left(1 + \frac{h}{h_s}\right) \exp\left(-8\frac{h^2}{h_s^2}\right), \tag{8}$$

that is valid for high h values. The approximation is shown in Figure 8 *(Right)* as the dashed dotted line. One can see that for the considered spectrum, and $h > 0.5\,h_s$, the accuracy of this spatial approximation is improved.

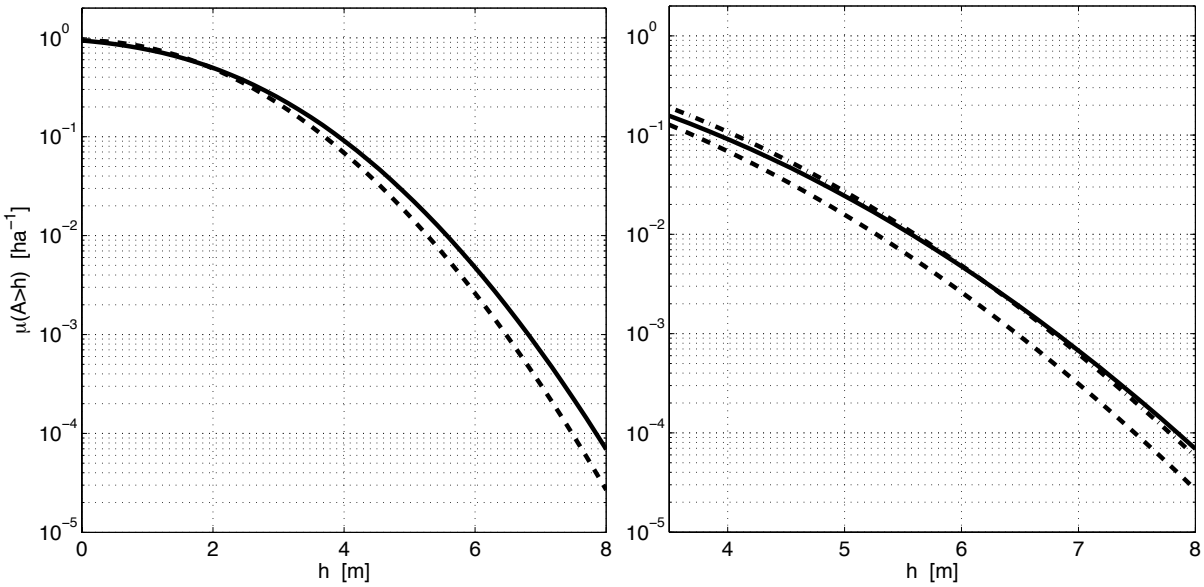

Figure 8: The logarithm of the intensity of waves in $W(x, y)$ with crest above h, $\mu(A > h)$. *Left:* logarithm of the intensity of waves in solid line, compared with the approximation based on the Rayleigh distribution given (7) in dashed line. *Right:* The enlarged left plot and with the added higher order asymptotic approximation (8) – dashed dotted line. The spectrum shown in Figure 2 *(Left)* is used for which the significant wave height is $h_s = 7$ [m].

4.4 The joint pdf of A, R and Θ.

We turn now to the joint density of crest height A, the distance to zero level contour R, and the angle Θ. We have chosen the region of high waves such that the crest hight A exceeds $0.5\, h_s = 3.5$ meter. The level $0.5h_s$ is chosen to be moderately high in order to allow comparisons with values of A, R, Θ obtained from simulated records. Using the solid lines given in Figure 8, one can roughly estimate that $P(A > 3.5) = 0.16/0.94$, which means that 17% of waves have crest exceeding $0.5\, h_s = 3.5$[m], which is sufficiently high to be see frequently in the records. As we mentioned before, for a long-crested sea instead of computed distribution, one can use the Rayleigh upper bound to assess how many wave is above the particular height. Namely, the probability that a crest exceeds h is bounded by the Rayleigh probability $\exp(-8(h/h_s)^2)$. Consequently, one concludes that in a long-crested sea, the fraction of wave crests above the threshold $0.5h_s$ is less than 13.5%.

In Figure 9, the marginal densities of R, A (left plot) and Θ, R (right plot) given that $A > 0.5\, h_s$, are presented. The densities are integrals of the joint pdf of A, R, Θ normalized by the probability $P(A > 0.5\, h_s)$. The levels of plotted contour lines are relative so that regions enclosed by the contour lines contain specified fractions of the total probability mass. Such a choice of level lines helps in visual evaluations of the accuracy of estimated joint pdf. More precisely, it enables comparisons with observed values of A, R, Θ shown as dots in the plots, since one can count fractions of dots included in the contours and compare those with the contour level defining fractions.

In order to check the accuracy of the numerical integrations involved in the computations of the densities shown in Figure 9, one thousand of waves were extracted (at random) from simulated surfaces $W(x, y)$. Since the probability that a crest is higher than $0.5\, h_s$ is 0.17 one expects to have 170 waves satisfying the condition $A > 0.5\, h_s$. Actually, there were 183 such waves with crest above the threshold. This exceeds the expected value 170 by about one standard deviation thus the difference is not significant.

For the extracted waves one has evaluated values of h, r and θ. The pairs (r, θ) were plotted as dots in the left plot and similarly pairs (θ, r) are shown as dots in the right plot. The isolines of the conditional pdfs are selected so that in the average there should be $180 \cdot x\%$ dots included in the contour.

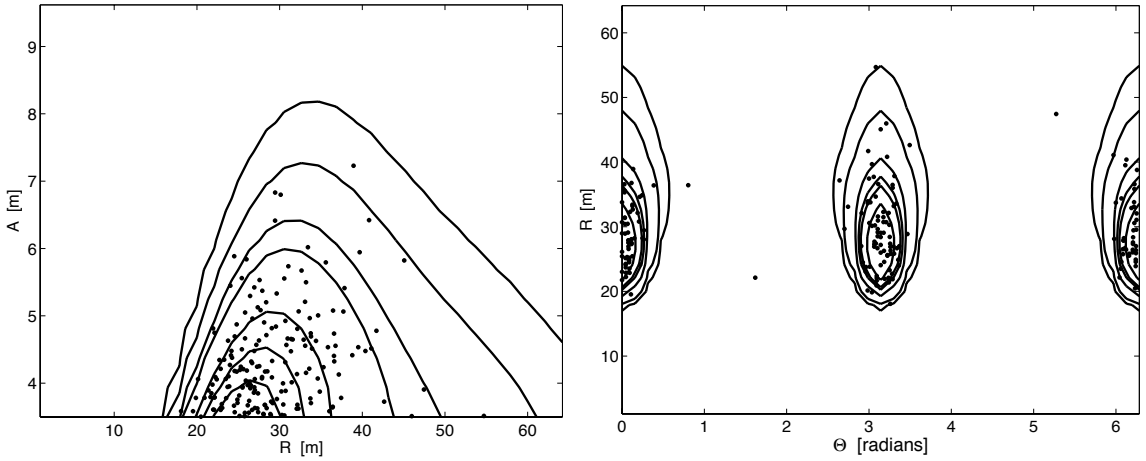

Figure 9: Conditional distributions given that crest is higher than $0.5\,h_s$ ($h_s = 7$ [m]). *Left:* The conditional joint pdf of the crest height A and the crest half-length R. *Right:* The conditional pdf of R and Θ. In the left plot contour lines contain 30%. 50%, 70% , 90%, 95%, 99%, 99.9% of the total probability while the contour lines in the right plot have the corresponding percentage set to 10%, 30%. 50%, 70% , 90%, 95%.

Fractions $x\%$ are specified in the figure. It is easier to count the point outside a contour line. This yields $0.001 \cdot 170 = 0.17, 1.7, 8.5, 17, 51, 85, \ldots$ expected dots outside the respective contour lines. In the left plot of Figure 9, one finds $0, 1, 9, 21, 61, 91, \ldots$ dots. Similarly in the right plot one expects to have $1.7, 8.5, 17, \ldots$ points outside the isolines while in the right plot $4, 8, 22, \ldots$ are counted. This confirms that the accuracy of the estimated densities is quite good.

Finally, we note that as the height of crest A is getting higher, the evaluation of the joint pdf of A, R and Θ by means of (26) is getting easier (and faster) since the indicator 1_B in the formula can be replaced by one, due to the asymptotic properties of the Gaussian fields. This is in contrast to using the simulation approach to approximate the pdfs involving A by counting frequencies – very high crests occur very seldom, see Figure 8, and computational cost of simulations increases.

4.5 Size of waves S

In Figure 6 *(Right)*, the pdf of the crest half-length R is shown. Variable R, defined in Definition 2, is the radius of the disk centered at a wave crest and underneath of the sea surface, see Figure 3 *(Right)*. Thus, the distribution of the disk's area D could be used to describe the spatial size of waves. The density of $D = \pi\, R^2$ is given by

$$f_D(s) = \frac{1}{2\sqrt{\pi\, s}} f_R\left(\sqrt{s/\pi}\right). \tag{9}$$

For the considered symmetric directional spectrum, the pdf of D (9) is shown in Figure 10 *(Left)*. The pdf is compared with the normalized histogram of D values extracted from simulations of field W. The plot demonstrates again very good accuracy of computed R-pdf.

It was mentioned in Section 3.2 that the area enclosed by ellipse S, defined in (5), could be a more adequate proxy describing waves geometry rather than the area of the disk D. In order to find the distribution of S, one can first to evaluate the pdf of crest lengths $\widetilde{R}$ evaluated in the standardized sea surface $\widetilde{W}(x, y)$ defined in (4). The density of S can be then computed by rescaling the disks by the mean half-wave lengths in the directions of the x and y axes via

$$f_S(s) = \frac{1}{2\sqrt{\pi L_x L_y\, s}} f_{\widetilde{R}}\left(\sqrt{s/\pi L_x L_y}\right). \tag{10}$$

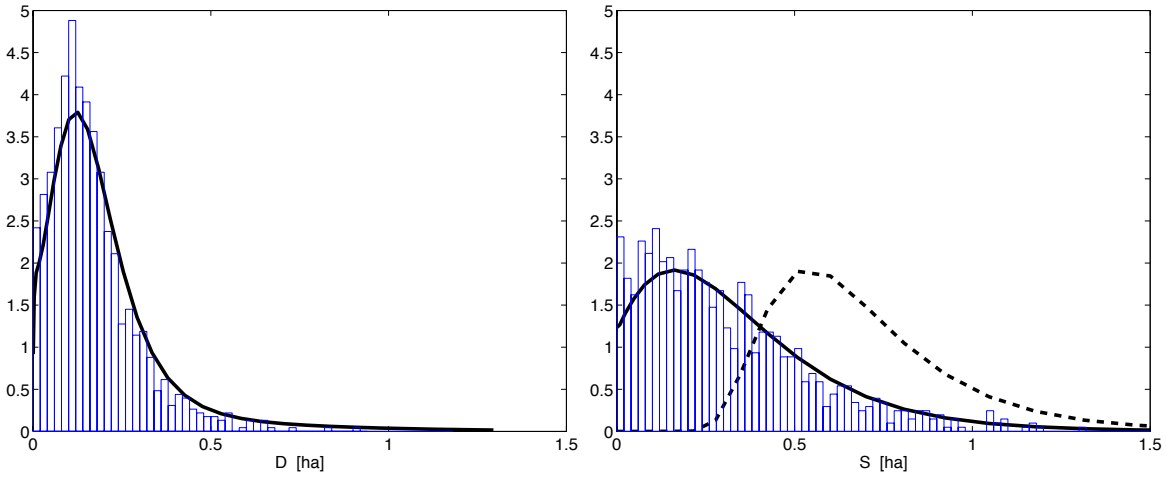

Figure 10: *Left:* Probability density of D [ha] (9) compared with the normalized histogram based on simulations. *Right:* Comparison of probability densities of S [ha], see (10), with the normalized histogram. The dashed line represents the conditional pdf of S given that the crest height exceeds $0.5\,h_s$.

The probability density of S is shown in Figure 10 *(Right)*. Comparison of the pdf with the normalized histogram of S confirms good accuracy of evaluated pdf of $\widetilde{R}$. From the plots given in Figure 10 one can conclude that the areas for ellipse S are statistically larger than the areas of disc D. Finally in Figure 10 *(Right)* the dashed line is the conditional pdf of S given that the crest height A exceeds $0.5\,h_s$. Not surprisingly one can observe that high waves also have large sizes.

5 Distributions of wave sizes for a confused sea

In this section we carry out similar computations to these presented in the previous section but this time for waves in a Gaussian sea having the directional power spectrum shown in Figure 2 *(Right)*. We limit ourselves to characteristics defined by the local maxima, i.e. according to Definition 2. The distributions of the crest half-length R, the direction of wave front Θ and the wave size S have been evaluated using the formula from Appendix II. We summarize our findings in Figure 11, where the pdfs (marginal and joint) analogous to the ones computed for the symmetric spectrum are presented. The spectrum similarly as before has the significant wave height $h_s = 7$ [m]. However, this time it is composed of two wave systems traveling in the x and y direction, respectively. The average crest length in the x and y directions $E[L_x], E[L_y]$, defined in (3), equal to 26π [m] and 31π [m], respectively. This results in short crested waves as seen in Figure 11 *(Top-Left)*. When comparing with the sea surface simulation shown in Figure 7, one can see that a superposition of waves coming from different directions leads to very irregular sea with many crests. Such a state of the sea is often referred to as a confused sea and our spectrum exemplifies such a state. The spectrum does not represent a realistic model of a sea spectrum and is chosen to illustrate the dependence of the wave characteristic on the spectrum shape. However, such compound sea spectra are of interest in reliability analysis of offshore structures, see e.g. [11]. The two wave system spectra are often occurring in the western Africa region when swells from southern and northern hemispheres storms meet, see [20].

As already mentioned, the discussed spectrum produces more crests. This can be validated by evaluating the crest intensity, which for the sea with asymmetric spectrum is 1.2 per hectare. This significantly larger than intensity 0.85 per hectare computed for waves with the symmetric spectrum shown in Figure 2 *(Left)*.

The joint density of R, Θ is shown in Figure 11 *(Top-Right)*. This distribution is also much different from the one shown in Figure 6 *(Left)* – in the current case the front waves are seen from all directions.

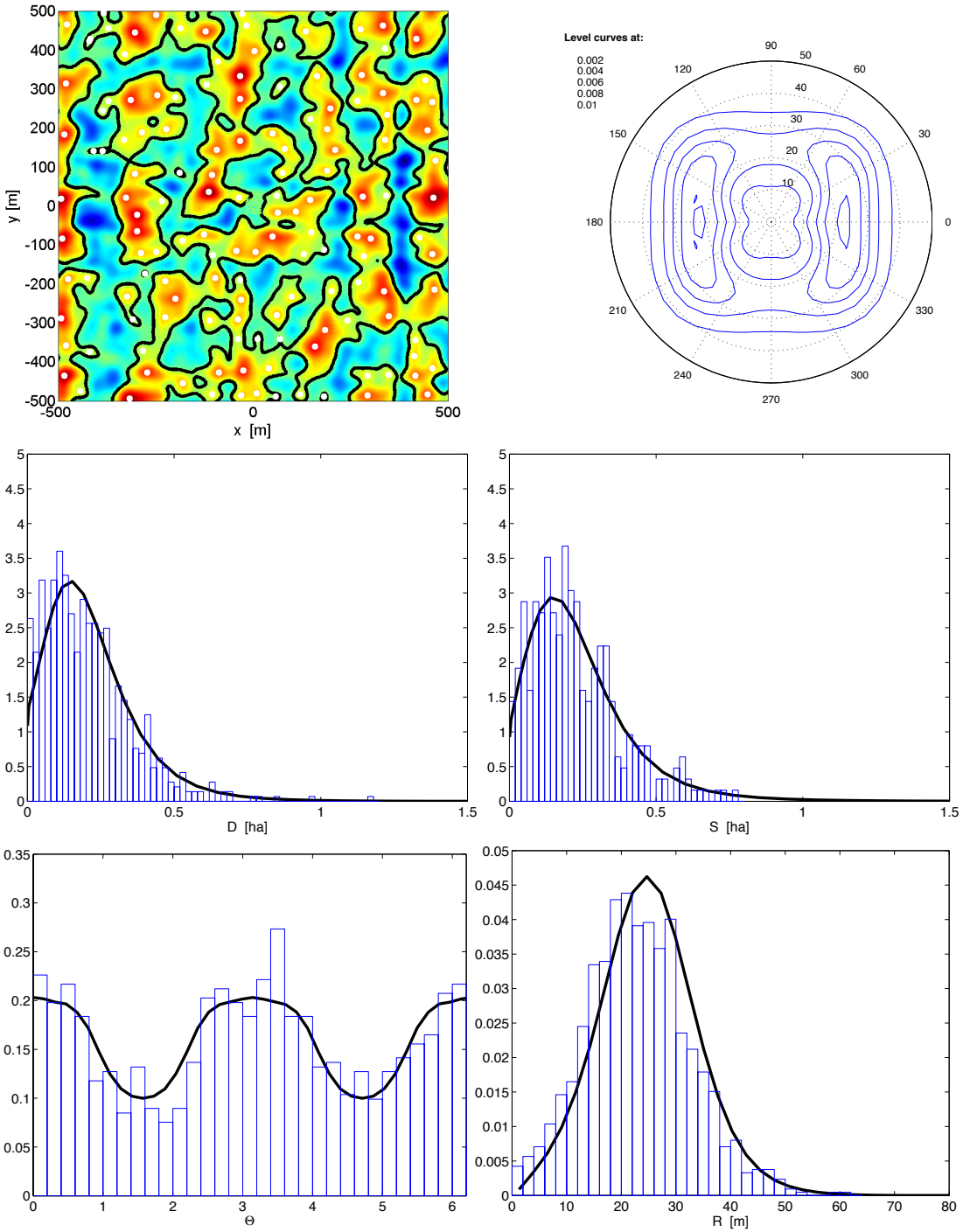

Figure 11: Results for the asymmetric spectrum example. *Top-Left:* Simulation of a Gaussian sea having the directional spectrum from Figure 2 *(Right)*. Positions of crests (positive local maxima) are marked as white dots. *Top-Right:* The joint probability density of R, Θ plotted in the polar coordinates, for waves defined in Definition 2. *Middle-Left:* The pdf of D [ha], see (9). *Middle-Right:* The pdf of S [ha], see (10). *Bottom:* The integrated pdfs from the joint pdf given in the top-right graph for Θ *(left)* and R *(right)*. The bottom and middle rows are also showing the corresponding histograms extracted from a simulated field.

Moreover, since $E[L_x] \approx E[L_y]$, then also the pdf of areas enclosed by the ellipses describing size of the waves, see Figure 11 *(Middle-Right)*, is now close to the distribution of disks areas D shown in Figure 11 *(Middle-Left)*.

Finally the marginal pdfs of R and Θ are evaluated by numerical integration of the joint pdf. In Figure 11 *(Bottom* the marginal pdf of R *(Right)* and the pdf of Θ *(Left)* are compared with the normalized histograms of R and Θ, respectively, found in simulated surfaces $W(x, y)$. One can see again that the histograms and pdfs $f_R(r)$, $f_\Theta(\theta)$ agrees very well showing the accuracy of the approach. Note that pdfs of Θ shown in Figures 6 *(Center)* and 11 *(Bottom-Left)* differ considerably. This illustrates the influence of the spectrum shape on the wave geometry in space.

Conclusions

A new method to measure size of waves in spatial sea surface records is presented. It is shown that the generalized Rice's formula can be used to evaluate the probability density functions of wave sizes in a Gaussian sea including the joint probability density of the crest height and the length of waves. The pdfs are given by explicit formulas but involving multidimensional Gaussian integrals. It is demonstrated that numerical integrations, using the methods available in MATLAB toolbox WAFO, give accurate approximations of the pdfs.

Acknowledgement

The first author acknowledges partial support by Swedish Research Council Grant Dnr: 2013-5180 and by Riksbankens Jubileumsfond Grant Dnr: P13-1024:1. The second author acknowledges partial support by Swedish Research Council Grant 340-2012-6004 and by Knut and Alice Wallenberg stiftelse.

References

[1] S. Åberg and I. Rychlik. Doppler-shift approximations of encountered wave statistics. *Ocean Engineering*, 34:2300–2310, 2007.

[2] S. Åberg, I. Rychlik, and M.R. Leadbetter. Palm distributions of wave characteristics in encountering seas. *Ann. Appl. Probab.*, 18:1059–1084, 2008.

[3] R. Adler. *The Geometry of Random Fields*. Wiley, New York, 1981.

[4] J. Allender, T. Audunson, S.F. Barstow, S. Bjerken, H.E. Krogstad, P. Steinbakke, L. Vartdal, L.E. Borgman, and C. Graham. The wadic project: A comprehensive field evaluation of directional wave instrumentation. *Ocean Engineering*, 16:505–536, 1989.

[5] J.-M. Azaïs and M. Wschebor. *Level Sets and Extrema of Random Processes and Fields*. Wiley, New York, 2009.

[6] A. Baxevani, K. Podgórski, and I. Rychlik. Velocities for moving random surfaces. *Probabilistic Engineering Mechanics*, 18:251–271, 2003.

[7] A. Baxevani and I. Rychlik. Maxima for gaussian seas. *Ocean Engineering*, 33:895–911, 2006.

[8] P.A. Brodtkorb. Evaluating nearly singular multinormal expectations with application to wave distributions. *Methodology and Computing in Applied Probability*, 8:65–91, 2006.

[9] P.A. Brodtkorb, P. Johannesson, G. Lindgren, I. Rychlik, J. Ryden, and E. Sjö. Wafo - a matlab toolbox for analysis of random waves and loads. In *Proceedings of the 10th International Offshore and Polar Engineering Conference*, volume III, pages 343–350, 2000.

[10] S. Gran. *A Course in Ocean Engineering*, volume 8 of *Developments in Marine Technology*. Elsevier Science Publishers, Amsterdam - London - New York - Tokyo, 1992.

[11] Z. Guede, M. Olagnon, H. Pineau, and Quiniou V. Francois, M. Fatigue analysis of an fpso under operational sea states with multimodal spectra. In *Proceedings of the ASME 2009 28th International Conference, OMAE*, volume 2 - Structures, Safety And Reliability, pages 301–307. ASME, 2009.

[12] M. Kac. On the average number of real roots of a random algebraic equation. *Bull. Amer. Math. Soc.*, 49:314–320, 1943.

[13] M.R. Leadbetter, G. Lindgren, and H. Rootzén. *Extremes and Related Properties of Random Sequences and Processes*. Springer-Verlag, 1983.

[14] M.R. Leadbetter, I. Rychlik, and K. Stambaugh. Estimating dynamic stability event probabilities from simulation and wave modeling methods. In *Proceedings of 12th International Ship Stability Workshop (ISSW2011)*, pages 147–154, 2011.

[15] G. Lindgren and I. Rychlik. Wave characteristic distributions for Gaussian waves, wave length, amplitude, and steepness. *Ocean. Eng*, 9:411–432, 1982.

[16] G. Lindgren and I. Rychlik. Slepian models and regression approximations in crossing and extreme value theory. *International Statistical Review*, 59:195–225, 1991.

[17] G. Lindgren, I Rychlik, and M. Prevosto. The relation between wave length and wave period in random gaussian waves. *Int. J. Offshore Polar Eng.*, 8:258–264, 1998.

[18] M.S. Longuet-Higgins. The statistical analysis of a random moving surface. *Phil. Trans. Roy. Soc. London, Series A*, 249:321–387, 1957.

[19] C. Mercadier. Numerical bounds for the distributions of the maxima of one- and two-parameter gaussian processes. *Adv. Appl. Prob.*, 2006.

[20] M. Olagnon, K. Ewans, G. Forristall, and M. Prevosto. West africa swell spectral shapes. In *ASME 2013 32nd International Conference on Ocean, Offshore and Arctic Engineering*, 2013.

[21] M. Olagnon and H. Krogstad. Observed short- and long-term distributions of wave steepness. In *Proc 8th Int Offshore Polar Engng Conference, Montreal*, pages 63–70, 1998.

[22] K. Podgórski, I. Rychlik, and U.E.B. Machado. Exact distributions for apparent waves in irregular seas. *Ocean Eng.*, 27:979–1016, 2000.

[23] S. O. Rice. The mathematical analysis of random noise. *Bell Syst Tech J*, 23(3):282–332, 1944.

[24] S. O. Rice. The mathematical analysis of random noise. *Bell Syst Tech J*, 24(1):46–156, 1945.

[25] I. Rychlik. A note on Durbin's formula for the first passage density. *Statistics & Probability Letters*, 5:425–428, 1987.

[26] I. Rychlik and M. R. Leadbetter. Analysis of ocean waves by crossing- and oscillation-intensities. In *Proceedings of the 7th ISOPE conference*, pages 206–213, 1997.

[27] J. Rydén, S. van Iseghem, M. Olagnon, and Rychlik I. Evaluating height-lenght joint distributions for the crest of ocean waves. *Applied Ocean Research*, 24:189–201, 2002.

[28] E. Sjö. Simultaneous distributions of space-time wave characteristics in a gaussian sea. *Extremes*, 4:263–288, 2001.

[29] U. Zähle. A general Rice formula, Palm measures, and horizontal-window conditioning for random fields. *Stochastic Processes and their Applications*, 17:265–283, 1984.

Appendix I: Gaussian sea

A zero mean Gaussian sea having directional spectrum $S(\omega, \alpha)$ can be approximated (with arbitrary accuracy) by a sum of independent cosine waves with Rayleigh distributed amplitudes and uniformly distributed phases. For the directional spectrum let $S_{jk} = S(\omega_k, \alpha_j)$ and define the field

$$W(x,y,t) \approx \sum_{\alpha_j \in [0,2\pi], \omega_k > 0} \sqrt{S_{jk}} R_{jk} \cos\left(t\,\omega_k - \frac{\omega_k^2}{g}(x\cos\alpha_j + y\sin\alpha_j) + \phi_{jk} \right) \sqrt{d\omega_k d\alpha_j}, \tag{11}$$

where R_{jk} are independent standard Rayleigh variables, ϕ_{jk} are independent uniformly distributed over $[0, 2\pi)$ phases that are also independent of R_{jk}, and $(d\omega_k, d\alpha_j)$ are infinitesimally small increments of the rectangular grid over arguments of the spectrum (the accuracy of approximation depends on how fine is the grid).

For $\mathbf{p} = (x_1, y_1, t_1)$ and $\mathbf{q} = (x_2, y_2, t_2)$, the covariance function is approximated by

$$\begin{aligned} C(W(\mathbf{p}), W(\mathbf{q})) &= \int_0^{2\pi} \int_0^{+\infty} S(\omega,\alpha) \cos\left(t\omega - \frac{\omega^2}{g} x\cos\alpha + y\sin\alpha \right) d\omega\, d\alpha \\ &\approx \sum_{\alpha_j \in [0,2\pi], \omega_k > 0} S_{jk} \cos\left(t\,\omega_k - \frac{\omega_k^2}{g}(x\cos\alpha_j + y\sin\alpha_j) \right) d\omega_k d\alpha_j, \end{aligned} \tag{12}$$

$x = x_2 - x_1$, $y = y_2 - y_1$ and $t = t_2 - t_1$.

Appendix II: Distribution of wave characteristics - Rice's method

For completeness we present expressions for the distributions of some wave characteristics obtained by means of various generalizations of Rice formula. The classical form of the latter yields an explicit form for the intensity of zeros in Gaussian process $W(t)$ having power spectral density $S(\omega) = \int S(\omega, \alpha)\, d\alpha$. If we restrict only to the upcrossings of the zero level, the average intensity (the average number of the uppcrossings per the time unit) is given by

$$\mu = \frac{1}{2\pi}\sqrt{\lambda_2/\lambda_0}. \tag{13}$$

Here λ_i's are spectral moments of $S(\omega)$. The formula can be reinterpreted as the intensity of waves defined by the zero upcrossing method. Despite that (13) is well known, let us mention a slightly more general version that extends its validity beyond the Gaussian case, i.e. one considers a zero mean stationary process $W(t)$ for which the expected number of times $W(t) = u$ in a region Λ, $N_\Lambda(u)$, say, is given by

$$E[N_\Lambda(u)] \;=\; \|\Lambda\| \int |z| f_{\dot{W}(0), W(0)}(z, u)\, dz. \tag{14}$$

Clearly, for the Gaussian case and due to independence between $\dot{W}(0)$ and $W(0)$, it turns to the classical Rice's formula originally presented in [12], [23] and [24]:

$$E[N_\Lambda(u)] \;=\; \frac{\|\Lambda\|}{\pi}\sqrt{\frac{\lambda_2}{\lambda_0}} e^{-u^2/2\lambda_0}. \tag{15}$$

Hence $\frac{1}{\pi}\sqrt{\frac{\lambda_2}{\lambda_0}}$ is the intensity of zeros, i.e. solutions of $W(t) = 0$. Since there are two zeros per wave yielding the formula for the intensity of waves (13). In what follows we present integral formulas used to approximate the quantities presented in Section 4. We comment on the principles used to derive the formula but we avoid mathematical technicalities and refer to other work for details.

We will start in Section AII.1 with the simplest problem of finding the intensity of waves in the time signal $W(t)$. The classical formula (15) will be used. Then we formulate a more general version of the

formula (18) and use it to obtain, in (21), a formula for the tail probability for the wave half-periods (lengths): $P(T^c > r)$.

In Section AII.2 Rice's formula (18) is extended to the sea surface $W(x, y)$ case, see (22), and then used to estimate for: the intensity of waves μ; the intensity that crest height exceeds h $\mu(A > h)$, see (23); and the intensity $\mu(A > h, R > r)$, see (25).

Derivations of formulas for joint probability densities of A, R, Θ require further generalizations of Rice's formula. We will not present those in this paper but in Section AII.3 we give the final results, the formulas for the pdf of (R, Θ) (28), (A, R, Θ) (26) and of (R_0, Θ_0) (29).

A II.1 Counting marked waves along lines

As mentioned above a "global" property that each second zero of $W(t)$ is an zero-upcrossing which marks front of a wave combined with Rice's formula gave the intensity of wave in (13). Finding distributions of wave characteristics is a harder problem since it requires accounting for some suitable local properties of $W(t)$ around a time t such that $W(t) = 0$. We will illustrate this "local" approach by providing a simple direct argument for the intensity of waves μ given (13).

Following the definition of waves presented in Figure 1, any zero upcrossing is a front of a wave. Obviously, if $W(t) = 0$ and

$$B = \text{"derivative } \dot{W}(t) \text{ is positive"} \tag{16}$$

is true, then at location t is a front of a wave. Another (more complex) example of local properties of $W(t)$ is

$$B_r = \text{"derivative } \dot{W}(t) \text{ is positive and for all } s \in [0, r],\ W(t + s) \geq 0\text{"}. \tag{17}$$

Again, if $W(t) = 0$ and B_r is true, then location t is a front of a wave having half-period longer than r. The expected values of zeros of W such that a condition "B" (or "B_r") holds can be computed using the following version of Rice's formula

Generalized Rice Formula: *If for a stationary Gaussian process W its marked zeros, i.e. times $W(t) = 0$ such that condition B holds, are homogeneously spread in time, then the expected number of marked zeros in Λ, $N_\Lambda(B)$ is given by*

$$E[N_\Lambda(B)] = \|\Lambda\| \int P(B|\dot{W}(0) = z, W(0) = 0)\, |z| f_{\dot{W}(0),W(0)}(z, 0)\, dz, \tag{18}$$

see Lemma 7.5.2 in [13] for more details.

Combining (18) with (16-17) one obtains formulas for intensity of waves μ and intensity of waves with half-period exceeding r, $\mu(T^c \geq r)$, respectively, viz.

$$\begin{aligned} \mu &= \int P(B|\dot{W}(0) = z, W(0) = 0))|z| f_{\dot{W}(0),W(0)}(z, 0)\, dz \\ &= \int_0^{+\infty} z f_{\dot{W}(0),W(0)}(z, 0)\, dz = \frac{1}{2\pi}\sqrt{\lambda_2/\lambda_0} \qquad (19) \\ \mu(T^c \geq r) &= \int P(B_r|\dot{W}(0) = z, W(0) = 0))|z| f_{\dot{W}(0),W(0)}(z, 0)\, dz, \qquad (20) \end{aligned}$$

and hence, by (6),

$$P(T^c \geq r) = 2\pi\sqrt{\lambda_0/\lambda_2} \int P(B_r|\dot{W}(0) = z, W(0) = 0))|z| f_{\dot{W}(0),W(0)}(z, 0)\, dz. \tag{21}$$

Note that derivation of (19) requires some simple calculus and employing property that $W(0)$ and $\dot{W}(0)$ are independent. (One also uses assumption that sea has zero mean.) Intensity $\mu(T^c \geq r)$ in (20) has to be evaluated using numerical integration. A function RIND from toolbox WAFO could be used for this purpose.

A II.2 Counting waves at a sea surface

In this section will consider similar problems as in Section AII.1 although this time a sea surface $W(x, y)$ will be considered instead of a record $W(t)$ in time or along a line. First formulas for intensity of waves μ, i.e. intensity of positive local maximums, and intensity of waves having crest A higher than h, i.e. $\mu(A > h)$, will be given. Both the problems were first studied by Longuet-Higgins in [18].

By Definition 2, a wave crest located at $\mathbf{p} = (x, y)$ exceeds level h ($A > h$) if for the sea surface gradient

$$(W_x(\mathbf{p}), W_y(\mathbf{p})) = (0, 0),$$

and the statement

$$B = \text{“matrix } \ddot{W}(\mathbf{p}) \text{ is negative definite and } W(\mathbf{p}) > h\text{”}$$

is true. The intensity $\mu(A > h)$ can be evaluated using the following version of Rice's formula.

Multivalued Rice Formula: *Consider a multivalued random functions $\mathbf{X}(\mathbf{p}) : R^n \to R^n$ such that at the point $\mathbf{p}$ a statement B about $\mathbf{X}$, its derivatives or any other random process is true. If zeros satisfying condition B are spread homogeneously in space then, under some conditions see e.g. [29], [3], [5], the following equation holds*

$$\mu(B) \quad = \quad \int P(B|\dot{\mathbf{X}}(\mathbf{0}) = \dot{\mathbf{x}}, \mathbf{X}(\mathbf{0}) = \mathbf{0})|\det \dot{\mathbf{x}}| f_{\dot{\mathbf{X}}(\mathbf{0}),\mathbf{X}(\mathbf{0})}(\dot{\mathbf{x}}, \mathbf{0})\, d\dot{\mathbf{x}}. \tag{22}$$

In order to utilize (22) for derivation the intensity of waves with crest above h, let us define $\mathbf{X}(\mathbf{p}) = (W_x(\mathbf{p}), W_y(\mathbf{p}))$ then

$$\mu(A > h) = \int_{\dot{\mathbf{x}} \text{ is neg. def.}} P(W(\mathbf{0}) > h|\dot{\mathbf{X}}(\mathbf{0}) = \dot{\mathbf{x}}, \mathbf{X}(\mathbf{0}) = \mathbf{0})|\det \dot{\mathbf{x}}| f_{\dot{\mathbf{X}}(\mathbf{0}),\mathbf{X}(\mathbf{0})}(\dot{\mathbf{x}}, \mathbf{0})\, \mathbf{d}\dot{\mathbf{x}}. \tag{23}$$

The so expressed intensity $\mu(A > h)$ has to be computed numerically and no explicit algebraic formula has been found yet. Even a formula for intensity of local maximums in $W(x, y)$, derived first in [18], is expressed using the Legendre elliptic integrals of the first and second kinds.

A II.2.1 Distribution and density of crest height A

By (6) the probability that wave crest observed at the sea exceeds h is given by

$$P(A > h) = \mu(A > h)/\mu(A > 0).$$

Differentiating (23) on h gives the pdf of A viz.

$$f_A(h) = c \int_{\dot{\mathbf{x}} \text{ is neg. definite}} |\det \dot{\mathbf{x}}| f_{\dot{\mathbf{X}}(\mathbf{0}),\mathbf{X}(\mathbf{0}),W(\mathbf{0}))}(\dot{\mathbf{x}}, \mathbf{0}, \mathbf{h})\, \mathbf{d}\dot{\mathbf{x}}, \tag{24}$$

where $c = 1/\mu(A > 0)$ is the normalization constant. The integral in (24) has to be computed numerically however for high values of h, which is often of the main interest, asymptotic formulas for $f_A(h)$ can be given, see [7], [5] and [19].

A II.2.2 Joint distribution of crest height and length A, R.

In this section we give formula for intensity of waves having crest height exceeding h and crest half-length longer than r, i.e. $\mu(A > h, R > r)$. Since for stationary sea surface $W(x, y) = W(\mathbf{p})$ waves having crest and length exceeding some fixed thresholds are homogeneously spread in space formula one can use (22) to evaluate $\mu(A > h, R > r)$, viz.

$$\mu(A > h, R > r) = \int_{\dot{\mathbf{x}} \text{ is neg. def.}} P(B|\dot{\mathbf{X}}(\mathbf{0}) = \dot{\mathbf{x}}, \mathbf{X}(\mathbf{0}) = \mathbf{0})|\det \dot{\mathbf{x}}| f_{\dot{\mathbf{X}}(\mathbf{0}),\mathbf{X}(\mathbf{0})}(\dot{\mathbf{x}}, \mathbf{0})\, \mathbf{d}\dot{\mathbf{x}}, \tag{25}$$

where

$$B = \text{“}W(\mathbf{0}) > h \text{ and for all } \mathbf{p} \in \mathcal{D}_r,\ W(\mathbf{p}) > 0\text{”}.$$

Here $\mathcal{D}_r$ is a disk centered at $\mathbf{0}$ having radius r. The integral in (25) has to be computed numerically. This is not an easy task since B is a function of infinitely many variables $W(\mathbf{p})$, $\mathbf{p} \in \mathcal{D}_r$ such that $W(\mathbf{p}) > 0$, and thus it has to be approximated by suitable discretization. For example, since a sea surface is often observed on a grid $\mathbf{p}_i$, say, then in practice the following is a natural approximation

$$B \approx \text{“}W(\mathbf{0}) > h \text{ and for all } \mathbf{p}_i \in \mathcal{D}_r,\ W(\mathbf{p}_i) > 0\text{”}.$$

Using the approximative definition of B, the integral in (25) becomes finite dimensional. Methods to evaluate numerically (22) have been discussed in several papers, see e.g. [16], [8]. The program RIND in WAFO [9] can be used to evaluate (23). Alternatively, one can use MC simulations (for example, Fourier snapshots methods are presented in [27]) to approximate the conditional probabilities $P(B|\cdot)$ and then numerically integrate the integrals in (22).

A II.2.3 Joint probability density of A, R, Θ

Derivation of the formula for joint pdf of A, R is quite complex. It involves generalizations of Rice's formula for non-homogeneously spread zeros of multivalued function $\mathbf{X}(\mathbf{p})$. In fact, it helps to introduce an additional variable Θ and derive a formula for the joint density of A, R, Θ, where Θ is a direction from the crest to the nearest point on the zero level contour. Here we give only the formulas without their derivations for the joint probability densities used to plot figures in Section 4.

It is convenient to consider the polar coordinates

$$\mathbf{p} = (r\cos\theta, r\sin\theta)$$

so that $W(r,\theta)$ is identified with $W(\mathbf{p})$. Next let us define an event

$$B = \text{“}W_{xx}(\mathbf{0}) < W_{xy}(\mathbf{0})^2/W_{yy}(\mathbf{0}),\ W_{yy}(\mathbf{0}) < 0 \text{ and for all } \mathbf{q} \in \mathcal{D}_r,\ W(\mathbf{q}) \geq 0\text{”}.$$

where $\mathcal{D}_r$ is the disk centered at $\mathbf{0}$ having radius r. Finally let 1_B be an indicator function of B equal one if B is true and zero otherwise. Then with

$$X(\mathbf{0},\mathbf{p}) = \Big(W_x(\mathbf{0}), W_y(\mathbf{0}), W_\theta(\mathbf{p}), W(\mathbf{p})\Big),$$

the joint pdf of A, R, Θ is given by

$$f(h,r,\theta) = \frac{1}{\mu(A>0)} E\left[J(r,\theta)1_B \left|\mathbf{X}(\mathbf{0},\mathbf{p}) = \mathbf{0}, W(\mathbf{0}) = h\right.\right] f_{\mathbf{X}(\mathbf{0},\mathbf{p}),W(\mathbf{0})}(\mathbf{0},h), \tag{26}$$

for the Jacobian

$$J(r,\theta) = W_{yy}(\mathbf{0})\left(W_{xy}^2(\mathbf{0}) - W_{xx}(\mathbf{0})\right)/W_{yy}(\mathbf{0})\left|W_{\theta\theta}(r,\theta)W_r(r,\theta)\right|, \tag{27}$$

where $W_{\theta\theta}(r,\theta)$, $W_r(r,\theta)$ are partial derivatives of $W(r,\theta)$. Clearly, $\mu(A>0)$ is equal to the intensity of waves given in (23). A special case of (26) is the joint pdf of R and Θ, viz.

$$f(r,\theta) = \frac{1}{\mu(A>0)} E\left[J(r,\theta)1_B \left|\mathbf{X}(\mathbf{0},\mathbf{p}) = \mathbf{0}\right.\right] f_{\mathbf{X}(\mathbf{0},\mathbf{p})}(\mathbf{0}), \tag{28}$$

where this time

$$B = \text{“}W(\mathbf{0}) > 0,\ W_{xx}(\mathbf{0}) < W_{xy}(\mathbf{0})^2/W_{yy}(\mathbf{0}),\ W_{yy}(\mathbf{0}) < 0 \text{ and for all } \mathbf{q} \in \mathcal{D}_r,\ W(\mathbf{q}) \geq 0\text{”}.$$

A II.2.4 Joint density of R_0, Θ_0

In this section, for comparison, we give formula for the pdf of R_0, Θ_0, i.e. the location, in the polar coordinates, of crest front closest to the origin as defined in Definition 1. The density is obtained using a generalization of the Durbin's formula for the first passage density for a process, see [25].

Let us define an event

$$B = \text{“for all } \mathbf{q} \in \mathcal{D}_r,\, W(\mathbf{q}) \geq 0\text{”}.$$

where $\mathcal{D}_r$ is the disk centered at $\mathbf{0}$ having radius r. Then with

$$X(\mathbf{p}) = \Big(W_\theta(\mathbf{p}), W(\mathbf{p})\Big),$$

the joint pdf of R_0, Θ_0 is given by

$$f(r,\theta) = 2\,E\left[J(r,\theta)1_B \left|\mathbf{X}(\mathbf{p}) = \mathbf{0}\right.\right] f_{\mathbf{X}(\mathbf{p})}(\mathbf{0}), \tag{29}$$

where $\mathbf{p} = (r\cos\theta, r\sin\theta)$ and the Jacobian is given, with the same notation as in (27), by

$$J(r,\theta) = \left|W_{\theta\theta}(r,\theta)W_r(r,\theta)\right|. \tag{30}$$

The formula presented in the last two subsections have been used in Figure 5, where for our example, the pdf of (R_0, Θ_0) computed using (29) (left plot) is compared with the pdf of (R, Θ) computed using (26) (right plot).

http://journals.lub.lu.se/stat

LUND UNIVERSITY
School of Economics and Management

Working Papers in Statistics 2016
LUND UNIVERSITY
SCHOOL OF ECONOMICS AND MANAGEMENT
Department of Statistics
Box 743
220 07 Lund, Sweden